Analysis of Coulomb and Johnsen-Rahbek electrostatic chuck performance in the presence of particles for EUV lithography

Sogard, Michael, Mikkelson, Andrew, Ramaswamy, Vasu, Engelstad, Roxann

Michael R. Sogard, Andrew R. Mikkelson, Vasu Ramaswamy, Roxann L. Engelstad, "Analysis of Coulomb and Johnsen-Rahbek electrostatic chuck performance in the presence of particles for EUV lithography," Proc. SPIE 7271, Alternative Lithographic Technologies, 72710H (17 March 2009); doi: 10.1117/12.815402

SPIE.

Event: SPIE Advanced Lithography, 2009, San Jose, California, United States

Analysis of Coulomb and Johnsen-Rahbek Electrostatic Chuck Performance in the Presence of Particles for EUV Lithography

Michael R. Sogard[a], Andrew R. Mikkelson[b], Vasu Ramaswamy[b], and Roxann L. Engelstad*[b]

[a]Nikon Research Corporation of America, 1399 Shoreway Road, Belmont, CA USA 94002-4107

[b]UW Computational Mechanics Center, Mechanical Engineering Department
1513 University Ave., University of Wisconsin - Madison, WI USA 53706-1572

ABSTRACT

The successful implementation of extreme ultraviolet lithography (EUVL) requires the use of an electrostatic chuck to both support and flatten the mask during scanning exposure. The EUVL Mask Standard, SEMI P37, specifies the nonflatness of the mask frontside and backside, as well as the thickness variation, to be 30 nm to 100 nm peak-to-valley, dependent on the class of substrate. Thus, characterizing and predicting the capability of the electrostatic chuck to reduce mask nonflatness to meet these specifications are critical issues. In this research, the ability of such chucks to deal with the presence of particles trapped between the substrate and chuck is investigated. Analytical and finite element modeling have been used to identify the forces needed to fully embed or deform a particle during electrostatic chucking. Simulation results (using an elastic analysis) have shown that the forces generated by both Coulomb and Johnsen-Rahbek chucks should be able to sufficiently deform, or flatten, particles which are nearly 1.0 μm in size.

Keywords: Extreme ultraviolet lithography (EUVL), EUVL reticle chucking, electrostatic chucking, particle chucking effects, finite element modeling

1. INTRODUCTION

The semiconductor industry will be facing a number of challenges in order to meet the image placement (IP) requirements in the sub-30-nm regime. In essence, all sources of IP error must be either minimized, compensated for, or completely eliminated. For extreme ultraviolet lithography (EUVL), one potential source of error is the nonflatness of the mask during exposure scanning. With nontelecentric illumination, any nonflatness of the patterned surface of the reticle will induce IP errors on the device wafer. Consequently, successful implementation of EUV lithography requires the use of an electrostatic chuck to both support and flatten the mask during exposure.

SEMI Standard P37-1102 specifies the frontside and backside flatness, as well as the low order thickness variation, to be between 30 nm and 100 nm peak-to-valley, depending on the class of substrate [1]. This standard is currently undergoing revision, and future flatness tolerances are expected to be tighter. Characterizing and predicting the capability of an electrostatic chuck to meet the flatness specifications are essential. This research focused on the response of the mask / chuck system in the presence of particles trapped within the interface. If particles are entrapped, they may increase reticle height variations, unless the chuck/reticle system can effectively flatten them.

* engelsta@engr.wisc.edu; phone: 608-262-5745; fax: 608-265-2316

Alternative Lithographic Technologies, edited by Frank M. Schellenberg, Bruno M. La Fontaine
Proc. of SPIE Vol. 7271, 72710H · © 2009 SPIE · CCC code: 0277-786X/09/$18 · doi: 10.1117/12.815402

The effects of entrapped particles are difficult to assess because the size, shape, number, and material properties of these contaminants are not always known. In addition, it is difficult to develop a model of a domain that is hundreds of millimeters in size, but contains sub-micron details. Figure 1 depicts a micron-sized particle entrapped between the substrate and chuck during electrostatic chucking. Surrounding the particle is a void, or gap, which may be millimeters in size. If the particle is not completely embedded or deformed, out-of-plane and in-plane distortions (OPD and IPD) will be seen on the patterned surface of the reticle. Determining the response of the individual components is challenging since the reticle substrate is 152 mm × 152 mm × 6.35 mm, particles are typically nanometers to microns in size, and chucking occurs over the mask Quality Area, which is 142 mm × 142 mm.

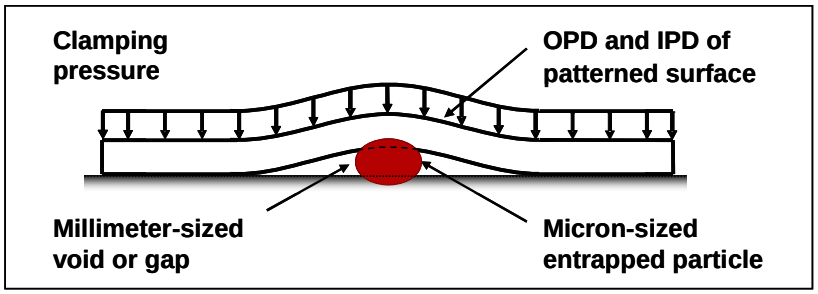

Fig. 1. Schematic illustrating electrostatic chucking of a substrate in the presence of a particle.

It is generally accepted that the problem must be divided into two regimes: the local response and the global response. Previous analyses have considered the local response for a spherical particle, including the determination of the elastic-plastic material properties [2-6]. The global response of the EUV mask has also been investigated to identify the final OPD and IPD of the pattern surface that result in image placement (IP) errors at the device wafer [3-6]. One of the goals of this research has been to establish the coupling relationship between the local and global models. Identifying the crushing ability of the various types of electrostatic chucks will aid in the assessment of overall chuck performance for the case of particle entrapment.

This research considers both Coulomb and Johnsen-Rahbek (J-R) electrostatic chucks. First, local modeling is used to determine the force needed to embed or deform the particle. Then global finite element (FE) models of the individual chucks are investigated to establish the force available for particle deformation as a function of the particle size. Coupling of the models is shown through various examples for particles up to 1.0 μm in size. Since larger particles also appear to be a concern, the FE models were modified and extended to illustrate how the loader arm with the mask carrier can be used to generate additional forces to facilitate the flatten of particles. Finally in the summary and conclusions, the elastic analysis completed here is summarized and an outline for future work is presented.

2. CHARACTERIZING THE LOCAL RESPONSE

Figure 2 shows a close-up of an entrapped particle, where application of the chucking pressure can cause embedding into the backside of the reticle or the top surface of the chuck, as well as deformation of the particle itself. In order to establish the force available for particle deformation, it is necessary to determine the effective particle height, *h*.

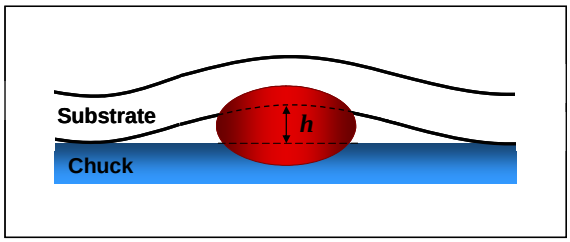

Fig. 2. Schematic of an entrapped particle during electrostatic chucking. The effective particle height, *h*, is the residual height of the particle after deforming and embedding.

The total amount of deformation and embedding of a particle (w_{total}) can be given by:

$$w_{total} = w_c + w_s + w_p \tag{1}$$

where w_c is the maximum deformation of the chuck surface, w_s is the maximum deformation of the substrate surface, and w_p is the maximum amount of deformation of the particle. The effective particle height can then be defined as:

$$h = H - (w_c + w_s + w_p) \tag{2}$$

where H is the original height of the undeformed particle.

For convenience, the particle was assumed to be cylindrical in shape so an analytical model could be used to identify each of the three components, w_c, w_s, and w_p. Previous investigations have shown that the shape of the particle is of little concern [2]. It should also be noted that it was assumed that all components would respond elastically, which represents a conservative approach for this initial work.

The embedding of the particle into the chuck can be modeled axisymmetrically as a rigid cylinder of radius R and height H indenting a homogenous elastic substrate as shown in Fig. 3. The force F is applied on top of the particle, and the substrate is assumed to be 362.5 µm in radius with a depth of 362.5 µm (which is large enough to ensure that boundary conditions will not affect the results for the size range of particles considered).

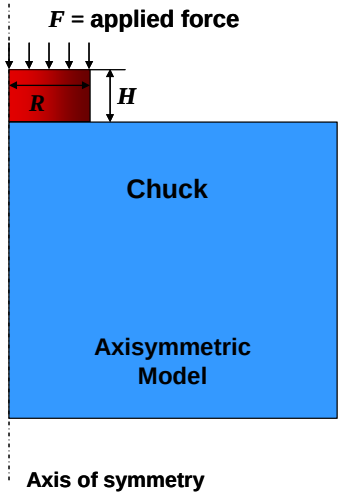

Fig. 3. Schematic of the analytical model to characterize particle embedding into the chuck.

The amount of embedding of the particle into the chuck (w_c) can be determined by [7,8]:

$$w_c = \frac{F(1-\nu_c^{\,2})}{2RE_c} \tag{3}$$

where E_c and ν_c are the elastic modulus and Poisson's ratio of the chuck substrate, respectively.

The embedding of the particle into the reticle with a backside layer can be modeled axisymmetrically as a rigid cylinder of radius R and height H indenting a homogenous elastic substrate with a thin film deposited on the backside surface as shown in Fig. 4. The force F is applied to the top surface of the particle, and the substrate assumed to be 362.5 μm in radius with a depth of 362.5 μm. It was assumed that the film had a thickness t of 60 nm.

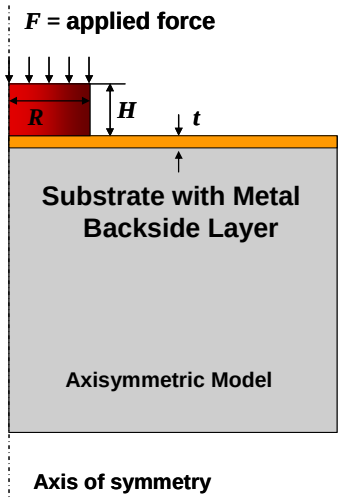

Fig. 4. Schematic of the analytical model to characterize particle embedding into the reticle with a thin film.

The amount of embedding of the particle into the substrate (w_s) with a thin film is given by [9]:

$$w_s = \frac{F}{4R}\left[1-\nu_s+(\nu_s-\nu_f)I_1\right]\left[\frac{(1-I_0)}{G_s}+\frac{I_0}{G_f}\right] \tag{4}$$

where the ν_s and ν_f are Poisson's ratio of the substrate and the film, respectively. The shear moduli (G_s and G_f) and elastic moduli (E_s and E_f) of the substrate and the thin film are related by:

$$G_f = \frac{E_f}{2(1+\nu_f)} \tag{5}$$

$$G_s = \frac{E_s}{2(1+\nu_s)}. \tag{6}$$

The weighting functions $I_0(\xi)$ and $I_1(\xi)$ can be expressed as:

$$I_0(\xi) = \frac{2}{\pi}\tan^{-1}\xi + \frac{1}{2\pi(1-\nu_s)}\left[(1-2\nu_s)\xi\ln\frac{1+\xi^2}{\xi^2} - \frac{\xi}{1+\xi^2}\right] \tag{7}$$

$$I_1(\xi) = \frac{2}{\pi}\arctan\xi + \frac{\xi}{\pi}\ln\frac{1+\xi^2}{\xi^2}. \tag{8}$$

Here $I_0(\xi)$ and $I_1(\xi)$ are functions of the normalized thickness ξ given by:

$$\xi = \frac{t}{R}. \tag{9}$$

Finally, the deformation of the particle (w_p) between the reticle and the chuck can be modeled as a cylinder of radius R, height H, and elastic modulus E_p under a uniformly distributed load as shown in Fig. 5.

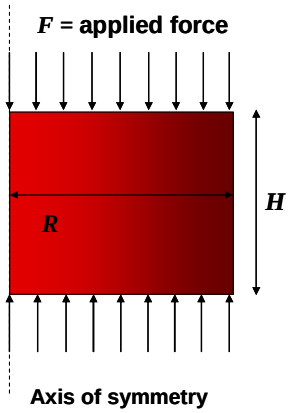

Fig. 5. Schematic of a particle deforming under a uniform distributed load.

The amount of deformation can be calculated using:

$$w_p = \frac{FH}{\pi R^2 E_p}. \tag{11}$$

The total amount of deformation and embedding of a particle, w_{total}, can be determined by substituting Eqs. (3), (4), and (11) into Eq. (1). Using the elastic properties of the individual components, the effective particle height (h) can be calculated as a function of the applied force for various initial particle heights (H).

To verify the analytical models, an axisymmetric finite element model was generated (see Fig. 6). The reticle substrate was assumed to be ULE® glass with a 60-nm backside coating of chrome. For convenience, the chuck and particle were assumed to be of the same material (ceramic-like). The elastic properties of these materials are listed in Table 1.

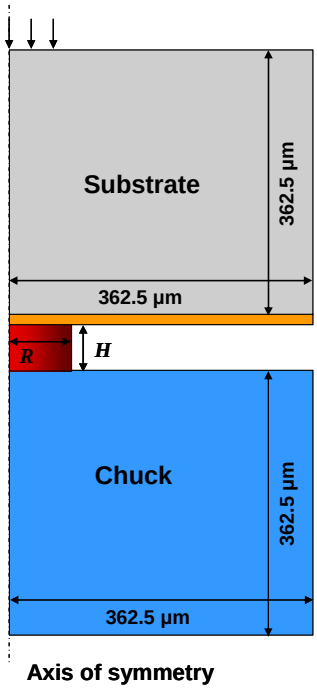

Fig. 6. Schematic of the axisymmetric FE model used to simulate particle deformation and embedding.

Table 1. Elastic material properties used in the FE local model.

Chuck	
Elastic modulus	100 GPa
Poisson's ratio	0.3
Reticle substrate	
Elastic modulus	66.3 GPa
Poisson's ratio	0.3
Metal Backside Layer	
Elastic modulus	250 GPa
Poisson's ratio	0.3
Particle	
Elastic modulus	100 GPa
Poisson's ratio	0.3

FE simulations were performed for three different initial particle heights, i.e., H = 0.1 µm, H = 0.5 µm, and H = 1.0 µm. For displaying the response results, the aspect ratio (H / R) of the cylindrical particle was varied between 0.5 and 2.0. The total applied load was distributed uniformly over a circular area on the top surface of the reticle as shown in Fig. 6. The radius of this area was varied to essentially match the original radius of the particle such that all of the applied force was utilized in deforming and / or embedding of the particle (i.e., the small area of load application is chosen so as to ensure that any contact occurring between the reticle and the chuck is purely a consequence of the particle becoming deformed and / or embedded). The total effective particle height at equilibrium is measured along the axis of symmetry as the difference between the original height of the particle and the sum of the total amount of particle deformation and the total amount of particle embedding into the backside of the reticle and the top surface of the chuck.

Figure 7 shows the comparison between the analytical and FE models for the three initial particle heights. The results predict the effective particle height as a function of the force applied to the particle. The plots show good correlation between the two predictions for all the cases, providing confidence in the analytical model. It should be noted that the models employ only elastic properties. In general, when the effective particle height becomes less than 50% of the initial height, the particle is no longer behaving as an elastic component and elastic-plastic deformations should be included. Consequently, extending the elastic analysis to effective heights of zero yields extremely conservative values for the force needed to completely embed and / or deform the particle. For example, a force much less that 0.155 N should be able to fully deform / embed a 1.0 µm particle, as shown in Fig. 7(c).

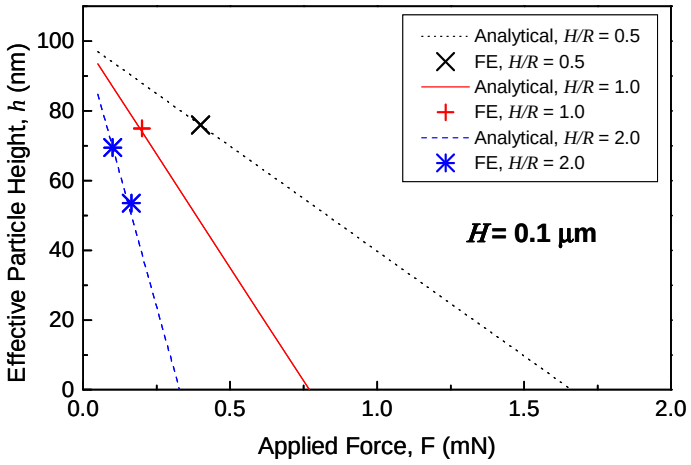

(a)

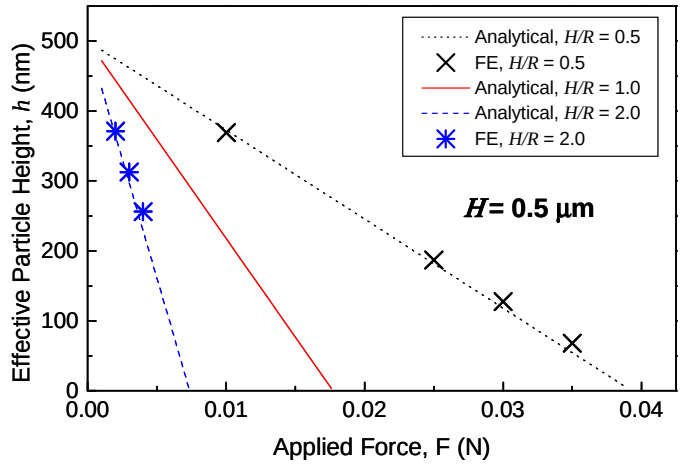

(b)

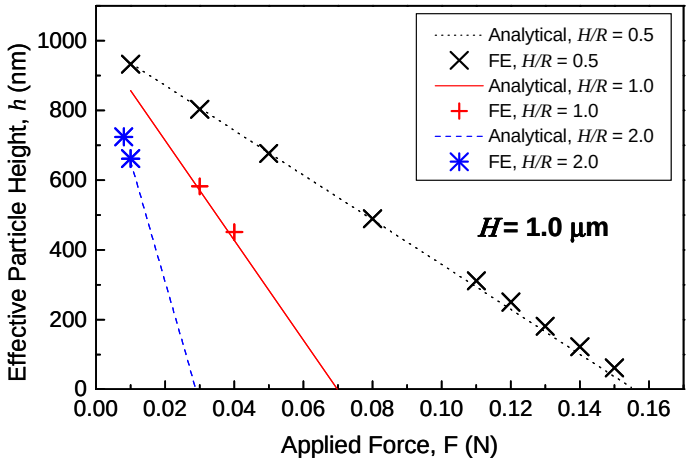

(c)

Fig. 7. Effective particle height as a function of applied force for initial particle heights of (a) 0.1 µm, (b) 0.5 µm, and (c) 1.0 µm. Results from both the analytical and FE models are shown for various aspect ratios of the particle dimensions.

3. CHARACTERIZING THE GLOBAL RESPONSE

In order to determine the magnitude of the available force, global modeling of the reticle / chuck system was used. Full three-dimensional (3-D) models of an EUVL mask and electrostatic pin chuck were generated. For the mask, it was assumed that the substrate was flat to within 50 nm, then the deposition of the multilayer caused a bow of 1.0 μm. To simulate entrapped particles, a single pin (or set of pins) on the chuck was modified by increasing the height slightly above the others. The chuck and pins were also assumed to be rigid.

For this study, a single pin at the center of the chuck was chosen. The additional height of the pin, *h*, essentially represents a deformed particle of that size resting on top of the centermost pin. As chucking is simulated and the electrostatic pressure is applied, the reticle is pulled toward the chuck. The reticle shape changes and reaches an equilibrium based on the number of pins in contact and the gap-dependent electrostatic forces. Since the local deformation of the reticle substrate by the pins is negligible in this case, the effective particle height is essentially equal to the increase in height of the patterned side of the substrate at the location of the particle, as shown in Fig. 8. The FE model calculates the force / pressure on each pin that is in contact with the reticle, as well as the gap radius.

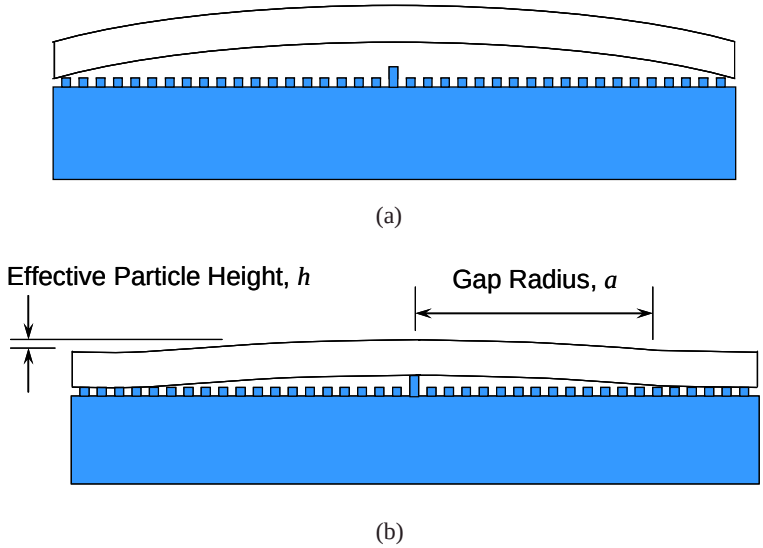

Fig. 8. Schematic of the FE model used for simulating either Coulomb or J-R electrostatic pin chucking. (a) Reticle bow of 1.0 μm before chucking with a single pin modified to simulate an entrapped particle. (b) Shape of the reticle after chucking illustrating the gap radius and effective particle height.

Both Coulomb and J-R electrostatic pin chucks were included in the analysis. Figure 9 illustrates the basic differences in the generation of electrostatic forces between the two chucks. In essence, for the Coulomb chuck, electrostatic pressure exists everywhere between the reticle and chuck. Consequently, the effects of nonflat substrates or the presence of particles have little effect on the clamping force, especially for gaps small compared to the dielectric thickness t_D. On the other hand, J-R forces depend on contact between the reticle substrate and dielectric material of the chuck. Large electrostatic forces can be generated at contact locations, but relatively weak forces are seen in gaps surrounding a particle. (Details describing the characteristics of these chucks have been presented in earlier publications [10]).

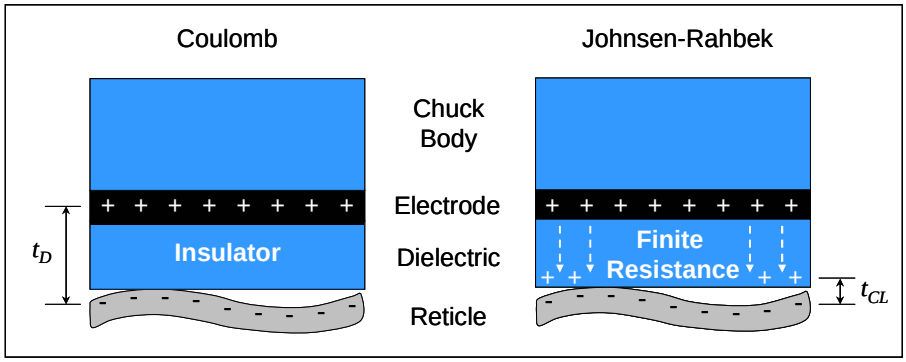

Fig. 9. Schematic of electrostatic force generation for the Coulomb and J-R chucks. Here t_D represents the dielectric layer thickness and t_{CL} is the contact layer thickness.

To be consistent, it was assumed that both chucks generated an average chucking pressure of 15 kPa (i.e., the average pressure with complete chucking). As previously stated, to ensure no deformations of the chuck occurred, both chucks were assumed to be rigid. In addition, both chucks utilized the same 12 × 12 pin array, which covered the Quality Area of the mask (i.e., 142 mm × 142 mm). Pin sizes were 2.5 mm × 2.5 mm with a height of 10 µm. This corresponded to a pin pitch of 12.67 mm and 4 % pin coverage. The chucking surface defined by the pin array was assumed to be flat, except for the modified pin in the center position. The low pin coverage puts the J-R chuck at a disadvantage, since its force generation requires contact between the chuck and reticle surfaces.

The results from the FE simulations for the Coulomb chuck are presented in Fig. 10(a). Here the available force represents the force seen on the center pin (with additional height h); this is the force a particle would have to support in order to result in that particular effective particle height. If a particle is not able to support that much force, it would be further deformed or embedded. The corresponding gap radius for the Coulomb chucking simulations is shown in Fig. 10(b). Since the pin spacing is over 10 mm, the values for the gap radius appear to be somewhat discontinuous on the plot.

Figure 11(a) shows the FE simulation results for the J-R chuck. Since the J-R force is essentially a contact force, it does not generate as much clamping force with a low pin density (such as this example case). The jumps in available force are associated with gap radii where the number of pins involved in contacting change abruptly. Consequently, the available force and the gap radius are highly dependent on pin layout and spacing. It should also be noted that for effective particle heights above 310 nm, the J-R forces begin to decrease because the corresponding gap radius is above 40 mm.

While the Coulomb chuck force is largely gap independent, the J-R force drops off significantly with increasing gap. For example, the parameters for each chuck were chosen so that the average chucking pressure was 15 kPa with complete chucking, i.e., when there was no residual gap between the reticle and chuck. However, the average pressure for the J-R chuck is severely reduced when there is a significant gap radius due to an entrapped particle. For this reason, a J-R chuck will most likely be operated at an average chucking pressure much higher than 15 kPa. Also, a pin surface is actually a disadvantage for a J-R chuck, since it requires some initial contact (in a region) to develop electrostatic forces (in that region). A continuous chuck surface (such as a slab chuck) would be a better fit for a J-R type force. J-R slab chucks are reported to have achieved average clamping pressures of up to 1.2 MPa [11].

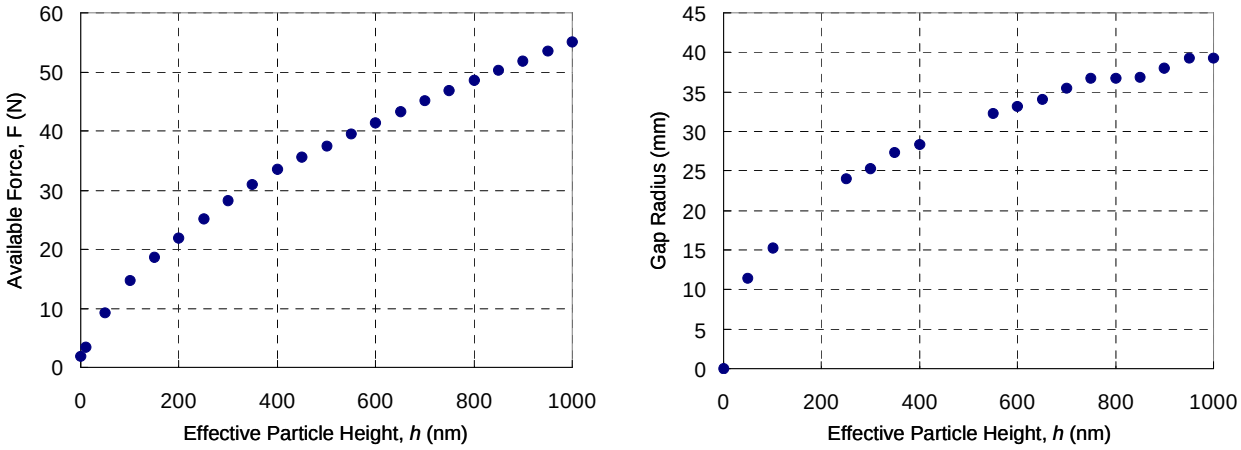

(a) (b)

Fig. 10. (a) Available force as a function of the effective particle height *h* for a Coulomb pin chuck. (b) Corresponding gap radius as a function of effective particle height *h* for the Coulomb pin chuck. The average pressure was 15 kPa.

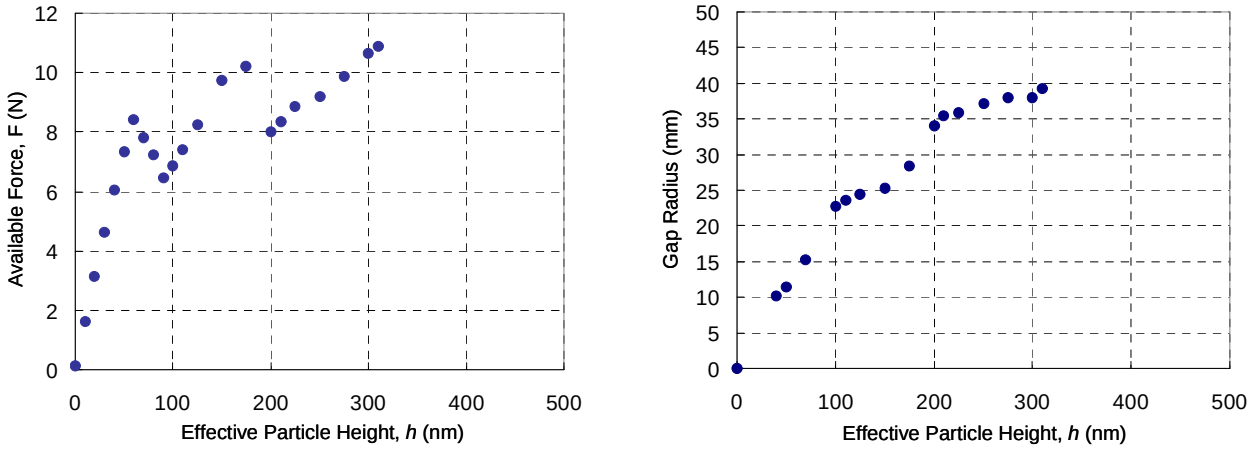

(a) (b)

Fig. 11. (a) Available force as a function of the effective particle height *h* for a J-R pin chuck. (b) Corresponding gap radius as a function of effective particle height *h* for the J-R pin chuck. The average pressure was 15 kPa.

4. COUPLING THE LOCAL AND GLOBAL MODELS

With the local model defining the force needed to fully embed and /or deform the entrapped particle, and the global model identifying the particle deforming force available, the coupling between the models can be seen on a combined graph as shown in Fig. 12. The log-log plot displays the family of curves from the local models where *H* equals 0.1

µm, 0.5 µm, and 1.0 µm for the three aspect ratios of H / R equal to 0.5, 1.0, and 2.0. Forces available for a particle located in the center are plotted for both the Coulomb and J-R pin chucks.

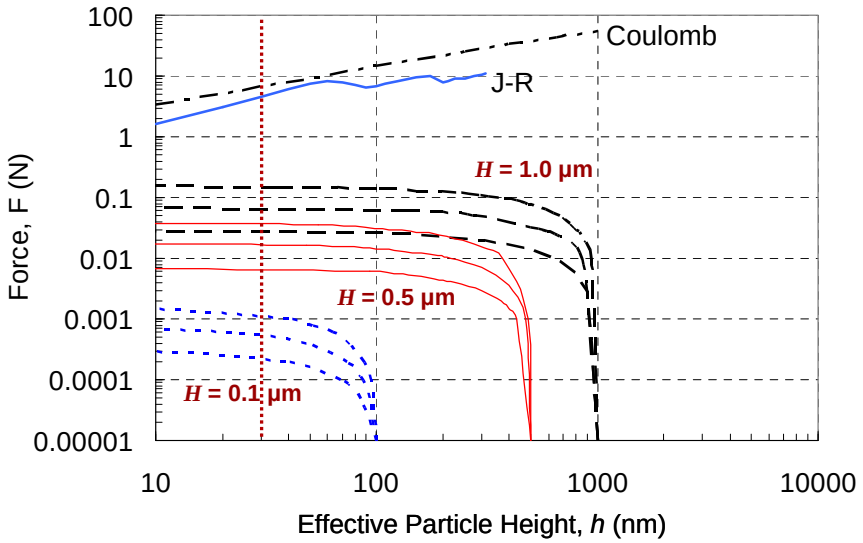

Fig. 12. Coupling the results from the local and global models. Effective particle heights should be kept below 30 nm to meet present standard specifications.

The chucking simulation results indicate that in order to flatten, or completely embed / deform, particles with initial heights up to 1.0 µm, a maximum chucking force of approximately 0.155 N is required. These particles are elastic, so if only half of the required force is available, the effective particle size will be half of the initial particle height. The available force for the Coulomb chuck over the range plotted is sufficient to deform or embed all particles for H values up to 1.0 µm. However, for the J-R chuck geometry used in this analysis, the force available to deform a particle starts to drop off for h values larger than 300 nm. While the J-R chuck can provide more than the 0.155 N needed to flatten a 1.0 µm particle, the force does not extend to large enough values of effective particle height to initially "capture" and flatten the undeformed particle. A chuck with higher pin density, or ideally, a slab chuck, would shift the drop off point to a larger h value. The force available to deform a particle on a Coulomb chuck will also drop off for h values somewhere between 1.0 and 2.0 µm. Since the Coulomb force doesn't drop off until h is larger than 1.0 µm, the Coulomb chuck will be able to fully deform / embed the range of elastic 1.0 µm particles considered and possibly some particles of sizes between 1.0 and 2.0 µm.

5. ADDITIONAL FLATTENING WITH RETICLE HANDLER

In the previous section, the success of a chuck in flattening particles depended on both the available deformation force of the chuck exceeding the maximum compliance force of the particle, and the chuck force exceeding the particle compliance force for the entire range of the particle effective height. The particle size plays a role as important as its maximum compliance force. If an auxiliary force could be used to compress a particle down to a size, or effective particle height, where the chuck force exceeded the compliance force, the chuck could "capture" the particle, and the auxiliary force could then be removed. This scenario was investigated by considering the mask handling system, which consisted of the mask carrier and the loader arm assembly.

The reticle is mounted on a mask carrier base plate (the bottom of the carrier), which is lifted up to the reticle chuck by an effector, or lifter arm, as shown in Fig. 13(a). After the chuck clamps the reticle, the carrier base plate is removed. Any additional force the lifter arm can apply to the reticle (above and beyond the weight of the reticle and carrier) during chucking may allow the chuck to successfully flatten larger particles. The mask carrier base plate was assumed to contact the reticle at the four corners, consistent with SEMI EUV Reticle Carrier Draft Document 4466. Placed on the carrier, gravity causes the bow of the reticle to increase from 1.0 µm (due to multilayer deposition) to 2.1 µm (illustrated in Fig. 13(b)).

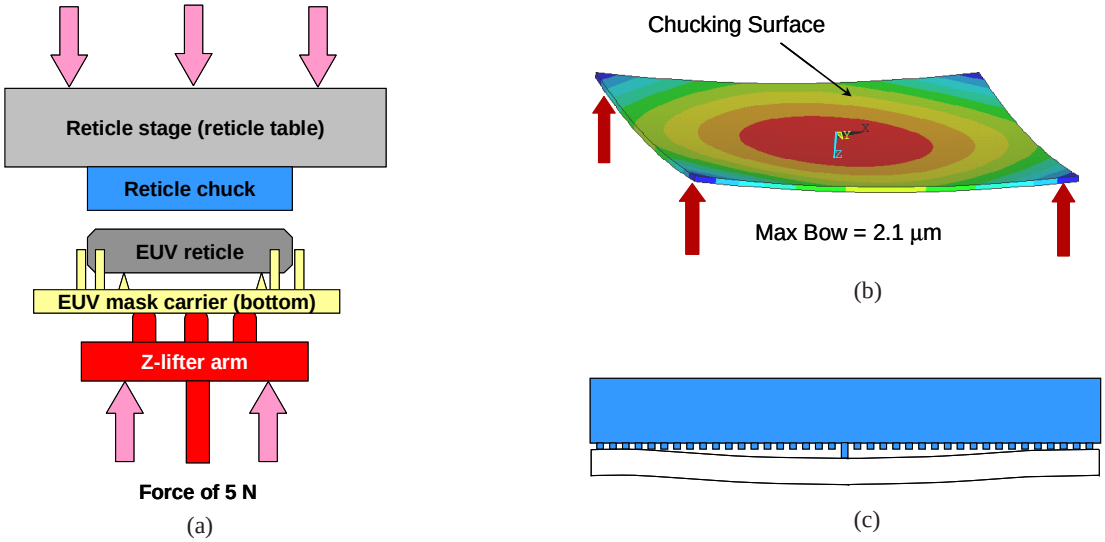

Fig. 13. (a) Conceptual design of the EUV mask carrier and lifter arm, which applies an additional loading force of 5 N. (b) Total reticle bow of 2.1 µm due to the stress in the multilayer and gravity. The effective force at each corner will be 1.25 N. (c) Reticle is loaded onto to the chuck in an inverted orientation. The center pin has been modified to identify additional loading available.

The carrier base plate was assumed to be rigid, so the distribution of forces on it from the lifter arm was not relevant. A total force of 5 N is assumed to be applied (over and above the weight of the carrier and reticle). For modeling, it was assumed that 1.25 N was applied at each of the four corners. This force is transferred through the reticle and presses the reticle against the chuck. Depending on the particle location(s) and size(s), this force might deform / embed particles before electrostatic forces are considered. A centrally located particle would only be affected if its initial size is 2.0 µm or larger (due to the reticle bow being 2.1 µm on the carrier). However, any particle of significant size near one of the corners would most likely be subjected to considerable force.

A 3-D FE model of the loading procedure was developed to determine the force on a centrally located particle as a function of particle height; this data is included in Fig. 14. The maximum available force is 5.0 N; this limit is based on the lifter arm and reticle chuck and stage system stiffness and could be increased in principle. Note that this force is available for any effective particle height exceeding roughly 5.0 µm. Thus it applies to particles of arbitrary size. The available force for a centrally located particle drops off as the corners of the reticle come in to contact with the chuck; in this case the 5.0 N is distributed between the particle and some of the pins. If the curve of available chuck force can be extended to larger effective particle heights, where it overlaps the available force from the lifter arm, the chuck can capture and flatten any particle whose maximum compliance force does not exceed the maximum available force from the combined chuck / lifter arm system. This may extend the chuck's tolerance for particles considerably.

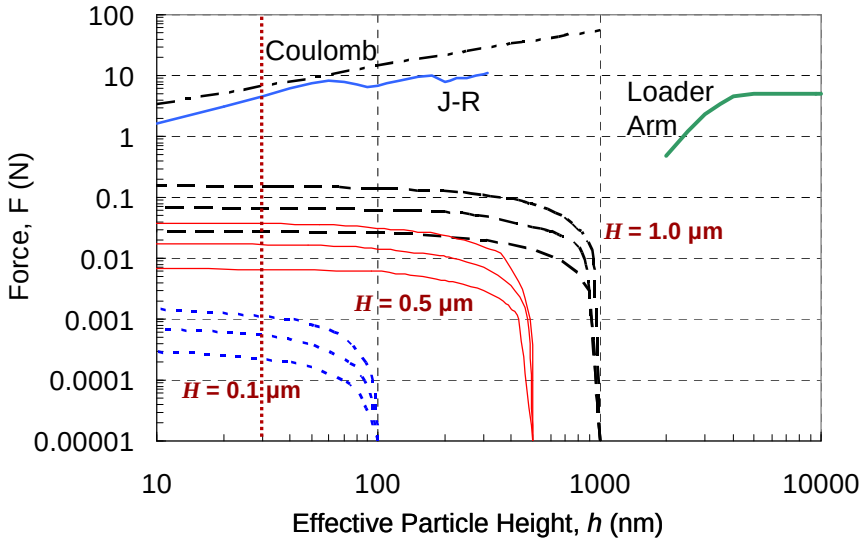

Fig. 14. Coupling the results from the local and global models, showing the additional force available with the loader arm from the mask carrier.

6. SUMMARY AND CONCLUSIONS

For EUV lithography, electrostatic chucking to support and flatten the reticle in the exposure tool will be a challenge, especially in the presence of particles. IP errors will be driven by the residual height of particles after they have been crushed and / or embedded into the reticle and chuck. In this study, both analytical and numerical models have been used to identify the forces needed to flatten, or fully crush or embed an entrapped particle as a function of the particle size. The analysis assumed elastic properties, therefore the results are somewhat conservative.

Full 3-D finite element models were developed to characterize the global response of the reticle / chuck system with a single particle positioned in the center of the mask. FE simulations have shown that the forces generated by both J-R and Coulomb electrostatic chucks should provide the force necessary to crush and / or embed particles up to nearly 1.0 µm in size. For much larger particles, a mask carrier with a loader arm could provide an additional force (5 N or even larger). However, particles between 1 to 3 µm may be a problem. This regime will be studied further.

Studies are underway to identify when it is sufficient to use an elastic analysis and when elastic-plastic deformations need to be considered. The analysis is also being extended to characterize the crushing forces needed in the presence of multiple particles.

ACKNOWLEDGMENTS

The authors would like to thank Nikon Corporation for supporting this research. The encouragement and support from Thomas Novak, Hidemi Kawai, Tsuneyuki Hagiwara, and Hajime Yamamoto is greatly appreciated.

REFERENCES

1. SEMI P37-1102, SEMI Standard Specification for Extreme Ultraviolet Lithography Mask Substrates.
2. Tejeda, R., Engelstad, R., Lovell, E. and Blaedel, K., "Particle-Induced Distortion in EUVL Reticles during Exposure Chucking," *Journal of Vacuum Science and Technology B*, Vol. 20, No. 6, pp. 2840-2843 (2002).
3. Ramaswamy, V., Engelstad, R., Turner, K., Mikkelson, A. and Veeraraghavan, S., "Distortion of Chucked Extreme Ultraviolet Reticles from Entrapped Particles," *Journal of Vacuum Science and Technology B*, Vol. 24, No. 6, pp. 2829-2833 (2006).
4. Ramaswamy, V., Mikkelson, A., Engelstad, R. and Lovell, E., "Predicting Wafer-Level IP Error due to Particle-Induced EUVL Reticle Distortion during Exposure Chucking," *Proceedings of SPIE's 25th Annual BACUS Symposium on Photomask Technology*, Vol. 5992, 59923T (2005).
5. Engelstad, R., Lovell, E., Mikkelson, A., Nataraju, M., Ramaswamy, V., Sohn, J., Dicks, G., Abdo A. and Tejeda, R., "Characterizing the Response of an EUV Reticle during Electrostatic Chucking," *Proceedings of the 22nd European Mask and Lithography Conference*, EMLC 2006, pp. 75-82 (2006).
6. Ramaswamy, V., Turner, K., Engelstad, R.and Lovell, E., "Predicting the Influence of Trapped Particles on EUVL Reticle Distortion during Exposure Chucking," *Proceedings of SPIE's 26th Annual BACUS Symposium on Photomask Technology*, Vol. 6349, 634938 (2006).
7. S. P. Timoshenko and J. N. Goodier, *Theory of Elasticity*, 3rd Edition, McGraw-Hill, Inc., New York, NY (1970).
8. R. W. Little, *Elasticity*, Prentice-Hall, Inc., Englewood Cliffs, NJ 357-358 (1973).
9. G. M. Pharr and H. Xu, "An Improved Relation for the Effective Elastic Compliance of a Film / Substrate System During Indentation by a Flat Cylindrical Punch," *Scripta Materialia*, Vol. 55, No. 4, pp. 315-318 (2006).
10. Sogard, M., Mikkelson, A., Nataraju, M., Turner, K. and Engelstad, R., "Analysis of Coulomb and Johnsen-Rahbek Electrostatic Chuck Performance for EUV Lithography," *Journal of Vacuum Science and Technology B*, Vol. 25, No. 6, pp. 2155-2161 (2007).
11. Ota, K., Taguchi, T., Amemiya, M., Nishiyama, Y., Kamono, T., Nishimura, N., Takikawa, T., Usui, Y. and Suga, O., "Experimental Evaluation of Out-Of-Plane Distortion of Electrostatically Chucked EUV Reticle," *Proc. of SPIE*, Vol. 6921, 69213S (2008).